miR-9-1 Is a New Circulating Biomarker for Higher-grade Meningioma Regulated via the EGFR-FOS Network

Daniele Baiz
University of Plymouth
Caterina Negroni
University of Plymouth
Sara Ferluga
University of Plymouth
Emanuela Ercolano
University of Plymouth
Claire L Adams
University of Plymouth
Agbolahan Sofela
University of Plymouth
David A Hilton
Plymouth Hospitals NHS Trust
Kathreena M Kurian
University of Bristol and Southmead Hospital - North Bristol Trust
C Oliver Hanemann (oliver.hanemann@plymouth.ac.uk)
University of Plymouth https://orcid.org/0000-0002-1951-1025

Research

Keywords: exosomes, meningioma, miR-9-1

Posted Date: August 5th, 2020

DOI: https://doi.org/10.21203/rs.3.rs-52124/v1

Abstract

Background: Meningiomas are the most common primary CNS tumors. According to the World Health Organization Classification (WHO), they are classified as benign (grade I), atypical (grade II), and anaplastic/malignant (grade III). Chemotherapy has proven ineffective in treating these tumors, which are primarily managed by surgery, radiotherapy, or a combination of them. Morbidity and mortality correlate with meningioma grade. Currently, risk assessment for treatment is based on the radiological assessment of tumor size, tumor growth rate, and/or clinical progression of symptoms.

Methods: We performed a cancer miRNA array in an *in vitro* model of meningioma in order to identify circulating biomarkers in meningioma patients. We validated the miRNA biomarker candidate in cells and tissues and analyzed its regulation. We then investigated expression in tissues and blood.

Results: We identified miR-9-1 as significantly overexpressed in atypical and anaplastic cells compared to benign. We further demonstrated that miR-9-1 overexpression is due to increased levels of FOS *via* upregulation of the EGFR receptor, and showed that miR-9-1 and FOS are upregulated in a cohort of higher-grade meningioma biopsies. Next, we isolated circulating exosomes from meningioma patients' serum samples, and found higher levels of miR-9-1 in higher-grade compared to low-grade meningiomas patients.

Conclusions: Overall, our study shows overexpression and the mechanism of miR-9-1 regulation and suggests miR-9-1 as a novel circulating biomarker candidate to identify tumor grade in meningioma.

Background

Meningioma is the most common primary central nervous system neoplasm originating from meningothelial cells. About a third of primary brain tumors in adults diagnosed every year in the UK is a meningioma (CBTRUS) (1,2). According to the World Health Organization (WHO), meningiomas are classified as benign (WHO I, ~80%), atypical (WHO II, ~15-20%) and anaplastic/malignant (WHO III, ~1-3%) (3). Meningiomas can cause mass effect on neural structures, resulting in focal neurological deficits, seizures, and death. They are usually relatively slow growing tumors and may reach a considerable size before patients present with symptoms, which depend on tumor location. Surgery and radiotherapy remain the mainstay of meningioma management, but complete tumor resection is not always possible due to inaccessible location of the tumor or proximity to eloquent structures, resulting in partial tumor control, and in meningioma recurrence (4). The 10-year progression free survival for grade I meningiomas is approximately 90%, about 50% for grade II and 0% in grade III meningiomas, irrespective of treatment modality; surgical excision, radiotherapy (including stereotactic radiosurgery) or a combination of both (5). Although research has identified several gene mutations, and the genetic background of meningioma is well characterized, our understanding of the molecular tumorigenesis of meningioma is still limited. Thus, the development of novel targeted therapies or diagnostic tools remains difficult (6-9).

MicroRNAs (miRNAs) represent a large class of small RNAs (~22 nucleotides) forming an emerging signaling network called “miRNome” (10). MiRNAs derive from larger precursor transcripts, are converted by several protein complexes into mature molecules in the cytosol (11), and regulate gene expression at the post-transcriptional level, playing an important role in many physiological and pathological processes, like cell proliferation, differentiation, apoptosis, carcinogenesis, and invasion (12,13). MiRNAs are also enriched in exosomes and micro-vesicles secreted by nearly all cells, including cancer cells, and circulating in many body fluids, including blood (14). Even though the mechanism is not fully understood, it is known that cells sort and load exosomes with a variety of potential biomarkers (proteins, miRNAs, mRNAs and lncRNAs), generating a specific pool reflecting the abnormalities present in the originating cells (15,16). Hence, a specific circulating miRNA signature can facilitate cancer diagnosis (17-19).

In the present study, using a cancer miRNA array, we discovered that the expression levels of miR-9-1 are increased in higher-grade meningioma. We found that miR-9-1 expression is regulated by the targetable Epithelial Growth Factor Receptor (EGFR) *via* the proto-oncogene FOS in meningioma. We confirmed that miR-9-1 is not only highly expressed in a cohort of atypical and anaplastic meningioma tissues compared to benign, but its levels are also increased in circulating serum exosomes derived from higher-grade meningioma patients. In summary we describe the mechanism of miR-9-1 upregulation and demonstrate that miR-9-1 is a novel potential circulating biomarker to discriminate between benign and higher-grade meningioma tumors.

Materials And Methods

Clinical samples

Meningioma (MN) specimens were collected following the national ethical approvals (REC No: 14/SW/0119; IRAS project ID: 153351) (Plymouth Hospitals NHS Trust: R&D No: 14/P/056 and North Bristol NHS Trust: R&D No: 3458), receiving a unique MN number. Blood was collected prior to surgery. ‘J’ specimens were collected via UK-Brain-Archive Information-Network (BRAIN UK; Ref no: 15/011; REC no: 14/SC/0098). Clinical and histopathological data for all samples used in this study are detailed in table 1.

Table 1. Clinical characteristics of the tumor samples used (n=130).

Clinical features	Group	Patients	
		n	(%)
Sex	Female	74	66.7
	Male	37	33.3
WHO grade	WHO I	81	62.4
	WHO II	37	28.4
	WHO III	12	9.2
Primary or recurrent	Primary	117	94.4
	Recurrent	7	5.6
Age at 1st diagnosis	Median	61	
	Range	20-87	

Cell culture

Human meningeal cells (HMC, cat# 1400) were obtained from Sciencell™, and maintained following the manufacturer's protocol. The malignant meningioma cell line KT21-MG1 (RRID:CVCL_M429) was cultured as previously reported (20). The benign meningioma cell line Ben Men-1 (RRID:CVCL_1959), and the malignant meningioma cell line IOMM-Lee (RRID:CVCL_5779) were both maintained as in (21). WHO I primary meningioma cells were obtained as reported in (22), and WHO II primary meningioma cells were isolated from resected tumors following the same protocol, but maintained in Dulbecco's Modified Eagle Medium F-12 Nutrient Mixture (Ham) (DMEM/F-12 (1:1)(1X) + GlutaMAX™-I; Thermo Fisher Scientific, Loughborough, UK) supplemented with 20% FBS (Sigma Aldrich, Gillingham, UK), 1% D-(+)-glucose (Sigma Aldrich, Gillingham, UK) and 100 U/mL penicillin/streptomycin (Thermo Fisher Scientific, Loughborough, UK).

RNA isolation, miRNA profiling, data mining tools, and gene expression

Total RNA was extracted using the Qiazol® reagent (Qiagen UK), following the manufacturer's protocol. RNA quality, integrity, and concentration were established using the NanoDrop ND-2000 (ThermoFisher Scientific UK).

Quantimir™ Cancer MicroRNA qPCR Array (Cambridge Biosciences) was performed according to the manufacturer's protocol. The bioinformatics analysis of the 96-miRNA profiling was performed using the NormFinder software (23) on an Excel 2016 platform (Microsoft, USA). Statistically significant miRNA candidates were identified by applying a Student's t-Test, assuming both equal and unequal variances ($p<0.01$). We selected only those candidates statistically significant in both groups, applying Venn analysis (Venny 2.1.0; http://bioinfogp.cnb.csic.es/tools/venny/index.html). Results were visualized by

hierarchical clustering using the software Morpheus®, applying the Euclidean distance metrics (https://software.broadinstitute.org/morpheus/index.html).

The RT² Profiler™ PCR Array Human EGF/PDGF Signaling Pathway and the RT² Profiler™ PCR Array Human miR-9 Targets (Qiagen) were performed according to the manufacturer's recommendations on a LightCycler® 480 II System (Roche).

RT-PCR was performed using 1 µg of total RNA using the TaqMan® MicroRNA Reverse Transcription Kit or the High-Capacity cDNA Reverse Transcription Kit (ThermoFisher Scientific UK), accordingly. Real Time PCR (qPCR) was conducted using the TaqMan® Fast Advanced Master Mix supplemented with TaqMan® assays (ThermoFisher Scientific UK) on a LightCycler® 480 II System (Roche), in triplicate, employing the following assays (ThermoFisher Scientific UK): hsa-mir-9* (ID 002231), hsa-mir-134-3p (ID 466606_mat), hsa-mir-145* (ID 002149), hsa-mir-10b* (ID 002315), hsa-mir-126 (ID 002228), FOS (Hs04194186_s1), CDH1 (Hs01023895_m1). As internal controls, we used RNU6B (ID 001093) or GAPDH (Hs02786624_g1), accordingly.

Gene expression levels were computed using the quantitative $2^{-(\Delta\Delta Ct)}$ method, employing the HMC as calibrator, in triplicate (24).

Proliferation and viability assays

Malignant meningioma KT21-MG1 and IOMM-Lee cells were plated in 96-well culture plates (3000 cell/well) for the proliferation assay, and in 6-well culture plates (3×10^5 cells/well) for the viability assay. Cells were allowed to adhere overnight (18 hours). The following day, medium was replaced with fresh warmed medium, and Afatinib was administered for 24 hours. Cell proliferation was assayed using the 'CellTiter-Glo® Luminescent Cell Viability Assay' as recommended by the supplier (Promega). Cell viability was determined by hemocytometer counting chamber using the trypan blue staining (Gibco).

Western blotting

Protein immunoblot was conducted as reported in (25). Briefly, tissues and cells were lysed using RIPA buffer supplemented with protease and phosphatase inhibitors (Roche and Santa Cruz Biotechnology, respectively). Protein concentration was estimated using the Pierce™ BCA Protein Assay Kit (Thermo Fisher Scientific) following the instructions of the supplier on a FLUOstar Omega microplate reader (BMG Labtech, Germany). Proteins were separated on a Laemmli SDS-PAGE, and transferred to a polyvinylidene difluoride membrane (Immun-Blot® PVDF Membrane, Bio-Rad). Membrane blocking, antibody incubation, and washes were performed as previously described (21).

The following primary antibodies were from Cell Signaling Technology: anti-c-FOS (#4384, RRID:AB_2106617), anti-CD9 (#13174, RRID:AB_2798139), anti-p-EGFR (#3777), anti-EGFR (#4267), anti-p-HER2/ErbB2 (#2247), anti-HER2/ErbB2 (#4290), anti-p-AKT (#4060), anti-AKT (#9272, RRID:AB_329827), anti-E-cadherin (#14472, RRID:AB_2728770) and anti-N-cadherin (#14215). Anti-CD63

(sc-59286, RRID:AB_784278) and anti-Calnexin (sc-46669, RRID:AB_626784) were purchased from Santa Cruz Biotechnology (USA), while anti-GM130 (clone 35, RRID:AB_398142) and GAPDH (#MAB374, RRID:AB_2107445) were from BD Biosciences (UK) and Millipore (USA), respectively. Detection was achieved using the ECL or ECL Plus Western Blotting substrate (Pierce). Membranes were exposed to Amersham Hyperfilm ECL (GE Healthcare Life Sciences). Immunoreactive bands were acquired at a resolution of 600 dpi, quantified using the ImageJ software, and each band was normalized *vs.* the corresponding GAPDH value.

Lentiviral-mediated transduction

KT21-MG1and IOMM-Lee cells were plated in 6-well plates at 1.5×10^5/well and left adhering O/N. Sub-confluent cells were washed once with PBS, and medium was replaced with complete medium supplemented with 8% protamine sulphate (Sigma-Aldrich). C-Fos shRNA (h) lentiviral particles (sc-29221-V, Santa Cruz Biotechnology) and Control shRNA Lentiviral Particles-A (sc-108080, Santa Cruz Biotechnology) were added according to the manifacturer's protocol. After 48h of incubation, medium containing lentiviral particles was removed, cells were washed once with PBS, and transduced KT21-MG1 and IOMM-Lee cells were selected for 4 days using 10 µg/mL puromycin (Thermo Fisher Scientific), before being assayed.

Exosome isolation

Ben-Men-1, KT21-MG1, and WHO I primary meningioma cells were cultured in medium supplemented with Exo-FBS™ Exosome-depleted FBS (System Biosciences). Briefly, cells were plated in 10-cm dishes at 1×10^6/well, and left adhering O/N. Then, medium was replaced, and cells were cultured for three days (see Fig. S7a). Supernatant was collected from confluent cells and exosomes were harvested using the Total Exosome Isolation (from cell culture media) reagent (Invitrogen, UK), following manufacturer's recommendations.

After whole blood collection in gold Vacutainer® tubes (Becton Dickinson, UK), specimens were allowed to clot undisturbed at room temperature for 30 minutes and serum was obtained by centrifuging at 2400 x g for 10 minutes at 4 °C. Exosome isolation from patients' serum samples was performed using the Total Exosome Isolation (from serum) Reagent (Invitrogen, UK) following manufacturer's instructions. Exosome enrichment was assessed by immunoblotting, performed using 40 µL of the exosomes resuspension, according to the Total Exosome RNA & Protein Isolation Kit (Invitrogen, UK) protocol.

Statistical analysis

Statistical and receiver operating characteristic (ROC) analyses were performed using the GraphPad Prism software. The unpaired Student's t-Test was applied in experiments with two different groups and the one-way ANOVA in experiments with three or more different groups, using the Tukey's multiple comparison as post-test. Data are expressed as mean ± SEM.

Results

miR-9-1 is overexpressed in high-grade meningioma cells

We analyzed the expression profile of 95 cancer miRNA genes by RT-qPCR array (Additional File 1) in the malignant meningioma KT21-MG1 cells (n=3), comparing their levels with the benign Ben-Men-1 (n=3), and tumor-derived (WHO I) primary meningioma cells (n=5). Stringent selection ($p<0.01$, see Fig. S1, S2, S3 in Additional File 2, and Additional File 3) and Venn analysis identified five significantly deregulated miRNA genes (Fig. S4a in Additional File 2) in KT21-MG1 cells (miR-9-1, miR-10b, miR-126, miR-145 and miR-134) (Fig. 1a, S4b-c in Additional File 2). As previously described (26), further validation *in vitro* confirmed the downregulation of miR-134 and -145 in KT21-MG1 cells (Fig. S4d, Additional File 2). However, we were unable to validate the expression levels of miR-10b and -126 (Fig. S4e, Additional File 2). Despite their levels in KT21-MG1 cells following those in the miRNA array described above, miR-10b and -126 expression levels were not validated in IOMM-Lee cells, a second *in vitro* model of malignant meningioma, when compared to Ben-Men-1. MiR-9-1 was the only candidate showing a consistent and significant upregulation in both malignant KT21-MG1 (11.66 folds) and IOMM-Lee (9.86 folds) cells, in keeping with the cancer miRNA array (KT21-MG1 = 9.90, Fig. 1b, Fig. 1c Ben-Men-1=1.67 folds) and primary cells (tumor-derived WHO I cells=2.89 folds; tumor-derived WHO II cells=4.56 folds). Indeed, we detected a consistent and significant increase of miR-9-1 expression levels with increasing meningioma grade, *in vitro,* using cell lines and primary cells (Fig. 1c). For grade III we used cell lines only, as primary cell cultures of grade III tumors are exceedingly rare.

FOS drives miR-9-1 overexpression via the EGFR pathway

Next, we focused on understanding which signaling pathway is driving miR-9-1 overexpression. Previous work by Chen and colleagues demonstrated that Erlotinib (a 1st generation and reversible EGFR inhibitor) inhibited the EGFR receptor in non-small cell lung cancer (NSCLC) cells, and reduced miR-9-1 levels, suggesting that the EGFR pathway plays a role in regulating miR-9-1 expression (27). We administered Afatinib (a 2nd generation irreversible EGFR and ERBB2 inhibitor) to KT21-MG1 and IOMM-Lee cells in a dose-dependent manner, confirming inhibition of malignant meningioma cells viability (Fig. S5a, Additional File 2) and proliferation, assessed by ATP assay (Fig. 5Sb, Additional File 2), and by monitoring the decrease of pAKTS473 levels by Western blotting (Fig. S5c, Additional File 2), when compared to vehicle. As shown in Figure 2a, Afatinib (AF) reduced phosphorylation of both EGFR-Y1068 and ERBB2-Y1248, when compared to vehicle, resulting in a significant reduction of miR-9-1 expression levels (AF 10 μM: 0.56 folds and 0.59 folds, respectively; AF 20 μM: 0.17 folds and 0.27 folds, respectively) in a dose-dependent manner (Fig. 2a). These results support the hypothesis that the EGFR pathway is involved in miR-9-1 regulation in malignant meningioma. We then conducted an EGF-PDGFR array profile in KT21-MG1 cells, by comparing the effects of 10 μM Afatinib (a dose that inhibits miR-9-1 expression similarly in both KT21-MG1 and IOMM-Lee cells) with vehicle, to identify the components of the EGFR pathway that control miR-9-1 expression in malignant meningioma cells (Fig. 2b). We observed that FOS was the only transcription factor significantly downregulated in KT21-MG1 cells following EGFR

inhibition both at the transcription (Fig. 2b-c) and protein levels (extending the analysis to IOMM-Lee cells, see Fig. 2a). Further analysis of FOS in meningioma cells showed that both KT21-MG1 and IOMM-Lee cells present significantly higher levels of FOS (and miR-9-1, see Fig. 1c), when compared to benign Ben-Men-1 cells (Fig. 2d; KT21-MG1=30.04 folds, IOMM-Lee=1.84 folds).

To demonstrate that EGFR activation leads to an increase of FOS, which results in increased miR-9-1, we stimulated KT21-MG1 and IOMM-Lee cells with EGF for 30 and 120 minutes (Fig. 3a) (22). Activation of the EGF receptor determined an increase in FOS levels (1.97 and 1.81 folds at 120 minutes, when compared to unstimulated KT21-MG1 and IOMM-Lee cells, respectively), and a significant increase of miR-9-1 (Fig. 3b; KT21-MG1=1.18 and 1.26 folds; IOMM-Lee=1.65 and 1.73 folds).

In order to further demonstrate that FOS was involved in miR-9-1 regulation, we performed a lentiviral-mediated silencing of FOS in both KT21-MG1 and IOMM-Lee cells (Fig. 3c). Decreased FOS was followed by a significant decrease in miR-9-1 expression (KT21-MG1=0.72 folds and IOMM-Lee=0.32 folds, respectively).

Next, we investigated what proteins could be affected by miR-9-1 overexpression in malignant meningioma. We performed a miR-9 targets array, comparing malignant KT21-MG1 to benign Ben-Men-1 cells, and we discovered that among the top putative targets of the miR-9-1, *CDH1* (E-cadherin) was the most significantly downregulated in KT21-MG1 cells (Fig. S6a, Additional File 2). We further confirmed *CDH1* repression at the mRNA (Fig. S6b, Additional File 2) and protein level (Fig. S6c, Additional File 2), in malignant KT21-MG1 and IOMM-Lee cells, when compared to benign Ben-Men-1 cells, and in anaplastic tumor biopsies (Fig. S6d, Additional File 2). Lower expression of E-cadherin detected in our tumor samples correlated with a more aggressive phenotype, and it was most likely responsible for a reduced cellular adhesion between tumor cells, leading to uncontrolled tumor growth and metastasis, as previously reported (28,29). Evaluation of E-cadherin expression levels after viral-mediated RNA interference of FOS in KT21-MG1 cells, showed significant increase of *CDH1* (Fig. S6e, Additional File 2). That was paralleled by a significant decrease of miR-9-1, as reported above in Fig. 3c.

In summary, these experiments demonstrated that miR-9-1 overexpression in malignant meningioma cells is related to EGFR-FOS activation.

miR-9-1 is overexpressed in higher-grade meningioma tissues

Following our *in vitro* results, we analyzed by RT-qPCR the expression levels of FOS and miR-9-1 in a discovery cohort of meningioma biopsies, assessing the correlation between the expression of FOS/miR-9-1 and meningioma grading. In line with our results *in vitro*, we showed that FOS expression is significantly increased in atypical and anaplastic meningioma tissues when compared to benign tumors (Fig. 4a; WHO II=2.26 Log_{10} folds, WHO III=2.16 Log_{10} folds). We also detected a significant upregulation of miR-9-1 in higher-grade meningioma tissues (Fig. 4b; WHO II=11.56 Log_{10} folds, WHO III=71.63 Log_{10} folds). Further analysis of miR-9-1 expression using receiver operating characteristic (ROC) analysis, showed that miR-9-1 has a high diagnostic value in discriminating between benign (WHO I) and atypical

(WHO II) meningioma tumors (AUC=0.8049, p<0.0001, 95% confidence interval 0.7162 to 0.8935). Furthermore, despite the small number of anaplastic (WHO III) tumors analyzed, ROC analysis suggested that miR-9-1 has a high diagnostic yield in differentiating between benign (WHO I) and anaplastic (WHO III) specimens (Fig. 4c; AUC=0.9136, p<0.0001, 95% confidence interval 0.8276 to 0.9995).

miR-9-1 is a potential circulating biomarker for higher-grade meningioma

After showing that miR-9-1 is upregulated in higher-grade meningioma tissues (when compared to those of benign origin, Fig. 4b-c), we extended this analysis to the exosomes cargo to evaluate whether miR-9-1 could be used as a non-invasive biomarker for higher-grade meningioma. As reported in Figure 5a, we initially evaluated the expression levels of miR-9-1 in an exosome enrichment assay, *in vitro*. We isolated extracellular exosomes released in the cell culture supernatant after three days of incubation, as described in Material and Methods (Fig. S7a, Additional File 2). We evaluated their enrichment and purification, by assessing the protein levels of CD63, CD9 and CD81 (exosome markers), and of Calnexin and GM130 (markers for endoplasmic reticulum -ER and Golgi, respectively) (30-32), as shown in the Western blot panel (Fig. 5a). Analysis of miR-9-1 expression levels in cell culture exosomes confirmed its upregulation in exosomes from malignant KT21-MG1 cells (5.92 folds, Fig. 5b), when compared to HMC, Ben-Men-1 (0.66 folds), and tumor-derived (WHO I) cells (2.16 folds). We then profiled a cohort of serum exosomes derived from meningioma patients, demonstrating that miR-9-1 is significantly upregulated (Fig. 5c, and S7b in Additional File 2) in serum exosomes derived from patients with atypical (WHO II, 8.10 Log_{10} folds) and anaplastic meningioma (WHO III, 11.99 Log_{10} folds), when compared to exosomes derived from WHO I meningioma patients. In addition, we performed a ROC analysis, which revealed that miR-9-1 holds high sensitivity and specificity for discriminating between benign (WHO I) and atypical (WHO II) (Fig. 5d; AUC=0.8056, p<0.001309, 95% confidence interval 0.6576 to 0.9536), and benign (WHO I) and anaplastic (WHO III) meningioma patients (AUC=0.9900, p<0.0008782, 95% confidence interval 0.9589 to 1.021).

Discussion

Meningioma is the most common primary central nervous system tumor originating from meningothelial cells (1,2). Despite its genetic landscape having been well characterized over the years, we still lack specific biomarkers and drug targets (33-36). Higher-grade meningiomas have significant morbidity and mortality.

Here we describe the mechanism of miR-9-1 upregulation and demonstrate that miR-9-1 is a novel potential circulating biomarker to discriminate between benign and higher-grade meningioma tumors.

Biomarkers are important in oncology, and are more recently including miRNas (18,37). A few studies have profiled meningioma tumors, suggesting potential circulating biomarkers, including miRNAs, that could advance cancer diagnosis and prognosis (26,38,39). Genome-wide array screening revealed that

miRNA clusters are implicated in meningioma tumorigenesis, correlating with proliferation and predicting recurrence of this disease (40). Some tumor-derived biomarkers can be found in body fluids, thus allowing quick and non-invasive patient testing. Differently to other brain tumors, meningiomas are located on the blood side of the blood brain barrier, thus they are more likely to secrete tumor-derived factors into the systemic circulation, whose discovery and employment as diagnostic tools could help with the clinical management of these tumors (41).

Our study has identified a novel biomarker, miR-9-1, significantly overexpressed in higher-grade meningioma tumors, and upregulated in serum exosomes from atypical and anaplastic meningioma patients. We analyzed benign, atypical and anaplastic/malignant cells, and identified miR-9-1 as a novel meningioma biomarker for higher-grade meningiomas. We confirmed its expression levels in a cohort of 130 biopsies, validating its overexpression in atypical and anaplastic tumors. Extending this analysis to a cohort of meningioma patients-derived serum exosomes, we have established that miR-9-1 is a potential circulating biomarker with a high diagnostic value for discriminating between benign and higher-grade tumors. According to the ROC analysis performed on meningioma tissues and serum exosomes from meningioma patients, miR-9-1 could have a high diagnostic value to discriminate between benign and higher-grade meningiomas. While a previous study identified a 6-miRNA signature in meningioma patients' serum (38), miRNAs in serum might not be associated with tumors, but could be a result of cell death and lysis, thus affecting their reliability as biomarkers. It has been shown that miRNAs in serum primarily exist inside exosomes, which are enriched in blood of cancer patients compared to healthy individuals (42). Therefore, by focusing our analysis on serum exosomes, we can more confidently say that the changes observed in miR-9 levels are due to tumor burden.

We also identified the EGFR pathway as driving miR-9-1 overexpression in malignant meningioma, *via* FOS, which is predicted to bind to the promoter/enhancer region of miR-9-1 (43). This is in keeping with previous studies, which have shown that EGF/ERBB2 receptors and FOS are upregulated, and are involved in the molecular process that drives meningioma pathogenesis and/or progression to higher-grade tumors (32,44-48). FOS knock out experiments supported this observation, resulting in decreased miR-9-1 and increased E-cadherin in malignant KT21-MG1 cells (49,50).

Conclusion

We identified the upstream EGFR-FOS signaling as responsible for miR-9-1 overexpression and E-cadherin downregulation in malignant meningiomas. In line with previously published studies, we suggest meningioma tumor progression is facilitated by enhanced EGFR/ERBB2 signaling *via* FOS, which leads to overexpression of miR-9-1 and translational repression of E-cadherin, facilitating tumor invasion, a distinctive feature of anaplastic/malignant tumors (29).

Altogether, our data show that miR-9-1 could be a novel circulating biomarker in meningioma patients, and a potential valuable tool to document EGF-R inhibition and to identify higher-grade tumors. Therefore,

miR-9-1 needs to be further evaluated with regards to its potential clinical role in monitoring meningioma patients.

Abbreviations

miR/miRNA microRNA

EGFR Epithelial Growth Factor Receptor

CNS Central Nervous System

WHO World Health Organization

CBTRUS Central Brain Tumor Registry of the United States

lncRNA Long Non-Coding RNA

HMC Human Meningeal Cells

FBS Fetal Bovine Serum

EGF Epidermal Growth Factor

PDGFR Platelet Derived Growth Factor Receptor

HER2/HerbB2 Human Epidermal Growth Factor Receptor 2

GAPDH Glyceraldehyde-3-Phosphate Dehydrogenase

DPI Dots Per Inch

PBS Phosphate Buffered Saline

shRNA Short Hairpin RNA

ROC Receiver Operating Characteristic

SEM Standard Error Of The Mean

NSCLC Non Small Cell Lung Cancer

AF Afatinib

CDH1 E-Cadherin

AUC Area Under The Curve

Declarations

Ethics approval and consent to participate: Meningioma (MN) specimens were collected following the national ethical approvals (REC No: 14/SW/0119; IRAS project ID: 153351) (Plymouth Hospitals NHS Trust: R&D No: 14/P/056 and North Bristol NHS Trust: R&D No: 3458), receiving a unique MN number. 'J' specimens were collected via UK-Brain-Archive Information-Network (BRAIN UK; Ref no: 15/011; REC no: 14/SC/0098).

Consent for publication: Not applicable.

Availability of data and materials: All data generated or analysed during this study are included in this published article (and its supplementary information files).

Competing interests: The authors declare no competing financial interests in relation to the work described and to have read and approved the final version of the manuscript.

Funding: This study was funded by Brain Tumour Research, the University of Plymouth and the FP7 Marie Curie Actions.

Author's contributions: DB: designed, executed and finalized the research, analyzed all data, wrote and revised the manuscript. CN and SF: contributed in executing the research. DB, CN, SF, EE, CLA: collected and processed clinical samples. AS and CLA: clinical data managing. DAH and KMK: clinical data managing and pathological characterization. COH: Acquired funding for and supervised the research and participated in writing the manuscript.

Acknowledgements: We are grateful to Dr. Jonathan Chernoff (Fox Chase Cancer Centre, Philadelphia, PA 19111-2497, USA) for donating the KT21-MG1-Luc5D cell line and the research nurses involved in this study. We would like to thank Prof. Matthias Futschik and Dr. Vasilis Lenis (School of Biomedical Sciences, Faculty of Health: Medicine, Dentistry and Human Sciences, University of Plymouth) for critical discussions about statistical analysis. Tissue samples were obtained from University Hospitals Plymouth NHS trust and Lancashire Teaching Hospitals NHS foundation Trust as part of the UK Brain Archive Information Network (BRAIN UK) which is funded by the Medical Research Council. We thank The Brain Tumor Research for supporting this work. CN was supported by a PUPSMD Postgraduate Research Award and DB was supported in part by the FP7 Marie Curie Actions (PCOFUND-GA-2012600181).

References

1. Wiemels J, Wrensch M, Claus EB. Epidemiology and etiology of meningioma. J Neurooncol. 2010;99(3):307-14.
2. Collins VP. Brain tumours: classification and genes. J Neurol Neurosurg Psychiatry. 2004;75 Suppl 2:ii2-11.

3. Louis DN, Perry A, Reifenberger G, von Deimling A, Figarella-Branger D, Cavenee WK, et al. The 2016 World Health Organization Classification of Tumors of the Central Nervous System: a summary. Acta Neuropathol. 2016;131(6):803-20.
4. Whittle IR, Smith C, Navoo P, Collie D. Meningiomas. Lancet. 2004;363(9420):1535-43.
5. Bi WL, Zhang M, Wu WW, Mei Y, Dunn IF. Meningioma Genomics: Diagnostic, Prognostic, and Therapeutic Applications. Front Surg. 2016;3:40.
6. Brastianos PK, Horowitz PM, Santagata S, Jones RT, McKenna A, Getz G, et al. Genomic sequencing of meningiomas identifies oncogenic SMO and AKT1 mutations. Nat Genet. 2013;45(3):285-9.
7. Clark VE, Erson-Omay EZ, Serin A, Yin J, Cotney J, Ozduman K, et al. Genomic analysis of non-NF2 meningiomas reveals mutations in TRAF7, KLF4, AKT1, and SMO. Science. 2013;339(6123):1077-80.
8. Smith MJ, Wallace AJ, Bennett C, Hasselblatt M, Elert-Dobkowska E, Evans LT, et al. Germline SMARCE1 mutations predispose to both spinal and cranial clear cell meningiomas. J Pathol. 2014;234(4):436-40.
9. Moazzam AA, Wagle N, Zada G. Recent developments in chemotherapy for meningiomas: a review. Neurosurg Focus. 2013;35(6):E18.
10. He L, Hannon GJ. MicroRNAs: small RNAs with a big role in gene regulation. Nat Rev Genet. 2004;5(7):522-31.
11. Bartel DP. MicroRNAs: target recognition and regulatory functions. Cell. 2009;136(2):215-33.
12. Fire A, Xu S, Montgomery MK, Kostas SA, Driver SE, Mello CC. Potent and specific genetic interference by double-stranded RNA in Caenorhabditis elegans. Nature. 1998;391(6669):806-11.
13. Bartel DP. MicroRNAs: genomics, biogenesis, mechanism, and function. Cell. 2004;116(2):281-97.
14. Lasser C, Alikhani VS, Ekstrom K, Eldh M, Paredes PT, Bossios A, et al. Human saliva, plasma and breast milk exosomes contain RNA: uptake by macrophages. J Transl Med. 2011;9:9.
15. Zhang J, Li S, Li L, Li M, Guo C, Yao J, et al. Exosome and exosomal microRNA: trafficking, sorting, and function. Genomics Proteomics Bioinformatics. 2015;13(1):17-24.
16. Anand S, Samuel M, Kumar S, Mathivanan S. Ticket to a bubble ride: Cargo sorting into exosomes and extracellular vesicles. Biochim Biophys Acta Proteins Proteom. 2019;1867(12):140203.
17. Esquela-Kerscher A, Slack FJ. Oncomirs - microRNAs with a role in cancer. Nat Rev Cancer. 2006;6(4):259-69.
18. Calin GA, Croce CM. MicroRNA signatures in human cancers. Nat Rev Cancer. 2006;6(11):857-66.
19. Kalluri R. The biology and function of exosomes in cancer. J Clin Invest. 2016;126(4):1208-15.
20. Chow HY, Dong B, Duron SG, Campbell DA, Ong CC, Hoeflich KP, et al. Group I Paks as therapeutic targets in NF2-deficient meningioma. Oncotarget. 2015;6(4):1981-94.
21. Bassiri K, Ferluga S, Sharma V, Syed N, Adams CL, Lasonder E, et al. Global Proteome and Phospho-proteome Analysis of Merlin-deficient Meningioma and Schwannoma Identifies PDLIM2 as a Novel Therapeutic Target. EBioMedicine. 2017;16:76-86.

22. Ferluga S, Baiz D, Hilton DA, Adams CL, Ercolano E, Dunn J, et al. Constitutive activation of the EGFR–STAT1 axis increases proliferation of meningioma tumor cells. Neuro-Oncology Advances. 2020;2(1).
23. Andersen CL, Jensen JL, Orntoft TF. Normalization of real-time quantitative reverse transcription-PCR data: a model-based variance estimation approach to identify genes suited for normalization, applied to bladder and colon cancer data sets. Cancer Res. 2004;64(15):5245-50.
24. Livak KJ, Schmittgen TD. Analysis of relative gene expression data using real-time quantitative PCR and the 2(-Delta Delta C(T)) Method. Methods. 2001;25(4):402-8.
25. Dunn J, Ferluga S, Sharma V, Futschik M, Hilton DA, Adams CL, et al. Proteomic analysis discovers the differential expression of novel proteins and phosphoproteins in meningioma including NEK9, HK2 and SET and deregulation of RNA metabolism. EBioMedicine. 2019;40:77-91.
26. Harmanci AS, Youngblood MW, Clark VE, Coskun S, Henegariu O, Duran D, et al. Integrated genomic analyses of de novo pathways underlying atypical meningiomas. Nat Commun. 2017;8:14433.
27. Chen X, Zhu L, Ma Z, Sun G, Luo X, Li M, et al. Oncogenic miR-9 is a target of erlotinib in NSCLCs. Sci Rep. 2015;5:17031.
28. Nagaishi M, Nobusawa S, Tanaka Y, Ikota H, Yokoo H, Nakazato Y. Slug, twist, and E-cadherin as immunohistochemical biomarkers in meningeal tumors. PLoS One. 2012;7(9):e46053.
29. Wallesch M, Pachow D, Blucher C, Firsching R, Warnke JP, Braunsdorf WEK, et al. Altered expression of E-Cadherin-related transcription factors indicates partial epithelial-mesenchymal transition in aggressive meningiomas. J Neurol Sci. 2017;380:112-21.
30. Thery C, Amigorena S, Raposo G, Clayton A. Isolation and characterization of exosomes from cell culture supernatants and biological fluids. Curr Protoc Cell Biol. 2006;Chapter 3:Unit 3 22.
31. Gyorgy B, Szabo TG, Pasztoi M, Pal Z, Misjak P, Aradi B, et al. Membrane vesicles, current state-of-the-art: emerging role of extracellular vesicles. Cell Mol Life Sci. 2011;68(16):2667-88.
32. Taylor DD, Shah S. Methods of isolating extracellular vesicles impact down-stream analyses of their cargoes. Methods. 2015;87:3-10.
33. Jung HW, Yoo H, Paek SH, Choi KS. Long-term outcome and growth rate of subtotally resected petroclival meningiomas: experience with 38 cases. Neurosurgery. 2000;46(3):567-74; discussion 74-5.
34. Rogers L, Gilbert M, Vogelbaum MA. Intracranial meningiomas of atypical (WHO grade II) histology. J Neurooncol. 2010;99(3):393-405.
35. Perry A. Unmasking the secrets of meningioma: a slow but rewarding journey. Surg Neurol. 2004;61(2):171-3.
36. Lam Shin Cheung V, Kim A, Sahgal A, Das S. Meningioma recurrence rates following treatment: a systematic analysis. J Neurooncol. 2018;136(2):351-61.
37. Almstrup K, Lobo J, Morup N, Belge G, Rajpert-De Meyts E, Looijenga LHJ, et al. Application of miRNAs in the diagnosis and monitoring of testicular germ cell tumours. Nat Rev Urol.

2020;17(4):201-13.
38. Zhi F, Shao N, Li B, Xue L, Deng D, Xu Y, et al. A serum 6-miRNA panel as a novel non-invasive biomarker for meningioma. Sci Rep. 2016;6:32067.
39. Kopkova A, Sana J, Machackova T, Vecera M, Radova L, Trachtova K, et al. Cerebrospinal Fluid MicroRNA Signatures as Diagnostic Biomarkers in Brain Tumors. Cancers (Basel). 2019;11(10).
40. Zhi F, Zhou G, Wang S, Shi Y, Peng Y, Shao N, et al. A microRNA expression signature predicts meningioma recurrence. Int J Cancer. 2013;132(1):128-36.
41. Erkan EP, Strobel T, Dorfer C, Sonntagbauer M, Weinhausel A, Saydam N, et al. Circulating Tumor Biomarkers in Meningiomas Reveal a Signature of Equilibrium Between Tumor Growth and Immune Modulation. Front Oncol. 2019;9:1031.
42. Gallo A, Tandon M, Alevizos I, Illei GG. The majority of microRNAs detectable in serum and saliva is concentrated in exosomes. PLoS One. 2012;7(3):e30679.
43. Fishilevich S, Nudel R, Rappaport N, Hadar R, Plaschkes I, Iny Stein T, et al. GeneHancer: genome-wide integration of enhancers and target genes in GeneCards. Database (Oxford). 2017;2017.
44. Hilton DA, Shivane A, Kirk L, Bassiri K, Enki DG, Hanemann CO. Activation of multiple growth factor signalling pathways is frequent in meningiomas. Neuropathology. 2016;36(3):250-61.
45. Rooprai HK, Martin AJ, King A, Appadu UD, Jones H, Selway RP, et al. Comparative gene expression profiling of ADAMs, MMPs, TIMPs, EMMPRIN, EGF-R and VEGFA in low grade meningioma. Int J Oncol. 2016;49(6):2309-18.
46. Arnli MB, Winther TL, Lydersen S, Torp SH. Prognostic value of ErbB2/HER2 in human meningiomas. PLoS One. 2018;13(10):e0205846.
47. Arnli MB, Meta R, Lydersen S, Torp SH. HER3 and HER4 are highly expressed in human meningiomas. Pathol Res Pract. 2019;215(10):152551.
48. Caltabiano R, Barbagallo GM, Castaing M, Cassenti A, Senetta R, Cassoni P, et al. Prognostic value of EGFR expression in de novo and progressed atypical and anaplastic meningiomas: an immunohistochemical and fluorescence in situ hybridization pilot study. J Neurosurg Sci. 2013;57(2):139-51.
49. Pecina-Slaus N, Cicvara-Pecina T, Kafka A. Epithelial-to-mesenchymal transition: possible role in meningiomas. Front Biosci (Elite Ed). 2012;4:889-96.
50. Araki K, Shimura T, Suzuki H, Tsutsumi S, Wada W, Yajima T, et al. E/N-cadherin switch mediates cancer progression via TGF-beta-induced epithelial-to-mesenchymal transition in extrahepatic cholangiocarcinoma. Br J Cancer. 2011;105(12):1885-93.

Figures

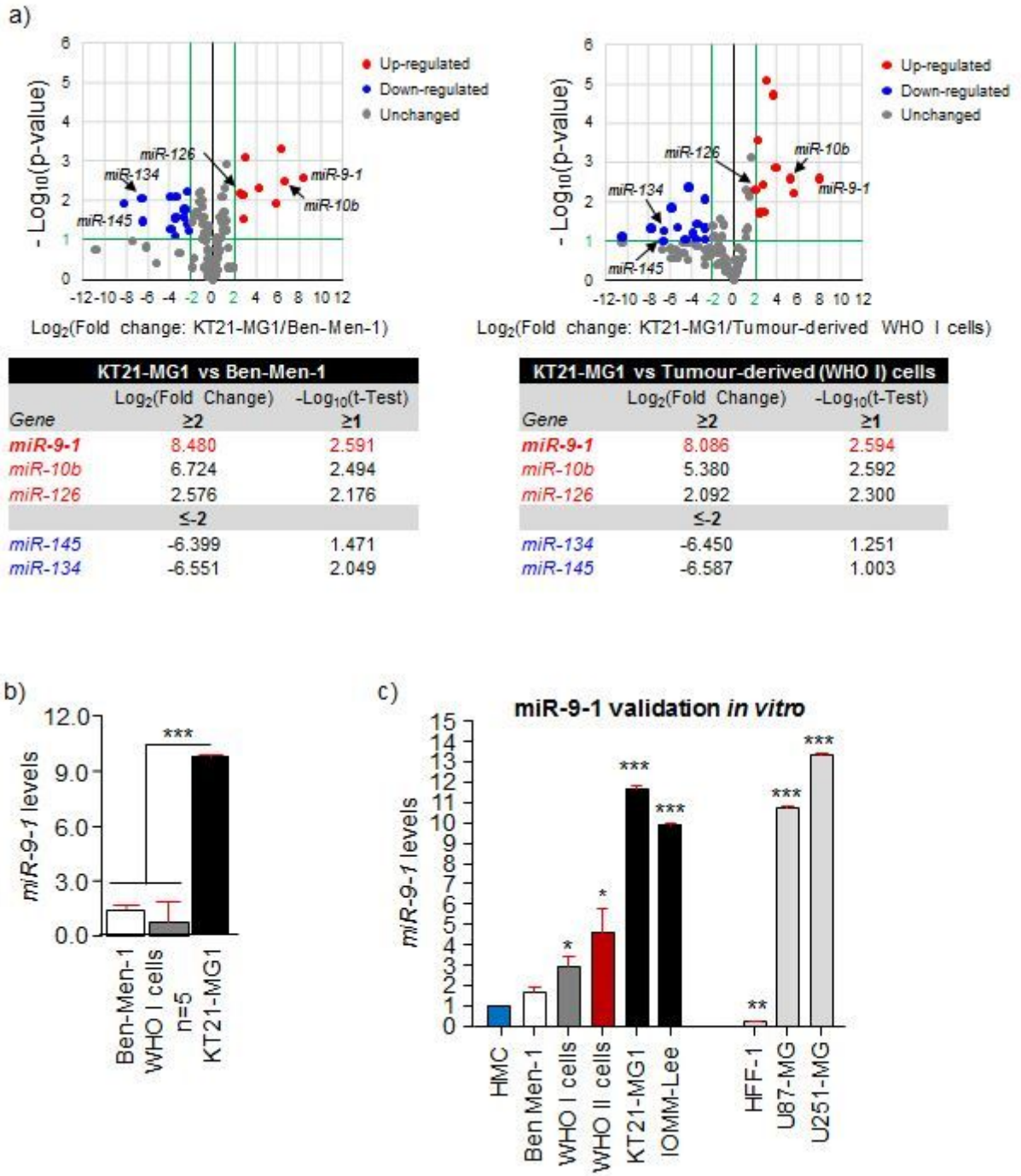

KT21-MG1 vs Ben-Men-1

Gene	Log_2(Fold Change)	$-Log_{10}$(t-Test)
	≥2	≥1
miR-9-1	8.480	2.591
miR-10b	6.724	2.494
miR-126	2.576	2.176
	≤-2	
miR-145	-6.399	1.471
miR-134	-6.551	2.049

KT21-MG1 vs Tumour-derived (WHO I) cells

Gene	Log_2(Fold Change)	$-Log_{10}$(t-Test)
	≥2	≥1
miR-9-1	8.086	2.594
miR-10b	5.380	2.592
miR-126	2.092	2.300
	≤-2	
miR-134	-6.450	1.251
miR-145	-6.587	1.003

Figure 1

MiR-9-1 is overexpressed in atypical and anaplastic meningioma, in vitro. a) Volcano plots reporting the Quantimir™ Cancer MicroRNA qPCR Array performed by profiling the malignant KT21-MG1 (n=3) meningioma cells versus benign Ben-Men-1 (n=3) and tumor-derived WHO I (n=5) cells. Results show the five miRNA genes (miR-9-1, miR-10b, miR-126, miR-145, miR-134), significantly deregulated in KT21-MG1 cells when compared to Ben-Men-1 and tumor-derived WHO I cells. Among these genes, miR-9-1 is significantly upregulated in KT21-MG-1 cells (p=0.0026, threshold p□0.01, when compared to the meningioma cells of benign origin above indicated). Green lines represent arbitrary threshold levels. b) MiR-9-1 levels in KT21-MG1 cells (9.90 Log2 folds, n=3) obtained from the Quantimir™ Cancer MicroRNA

qPCR Array and plotted versus Ben-Men-1 (1.41 Log2 folds, n=3) and tumor-derived WHO I cells (0.77 Log2 folds, n=5). Data are expressed as mean Log2 (2-ΔΔCt) ± SEM, ANOVA one-way (***p<0.001), when compared to benign cells. c) Validation assay of miR-9-1 performed by RT-qPCR shows that its expression significantly increases with increasing meningioma grades, when compared to HMC cells (n=3, mean=1). Ben-Men-1 cells (benign, n=3; mean=1.67); tumor-derived WHO I cells (benign, n=8; mean=2.89); tumor-derived WHO II cells (atypical, n=7; mean=4.56); KT21-MG-1 cells (anaplastic, n=3; mean=11.66); IOMM-Lee cells (anaplastic, n=3; mean=9.86). Negative control: human fibroblast cells (HFF-1, n=3; mean=0.21). Positive controls: U87-MG cells (n=3, mean=10.69), U251-MG (n=3, mean=13.38). Data are expressed as mean ± SEM, Student's t-Test (*p<0.05), ANOVA one-way (**p<0.005, ***p<0.001), when compared to Ben-Men-1 cells. All cell lines (HMC, Ben-Men-1, KT21-MG1, IOMM-Lee, HFF-1, U87-MG, and U251-MG) were profiled at three different passages, to ensure gene expression consistency.

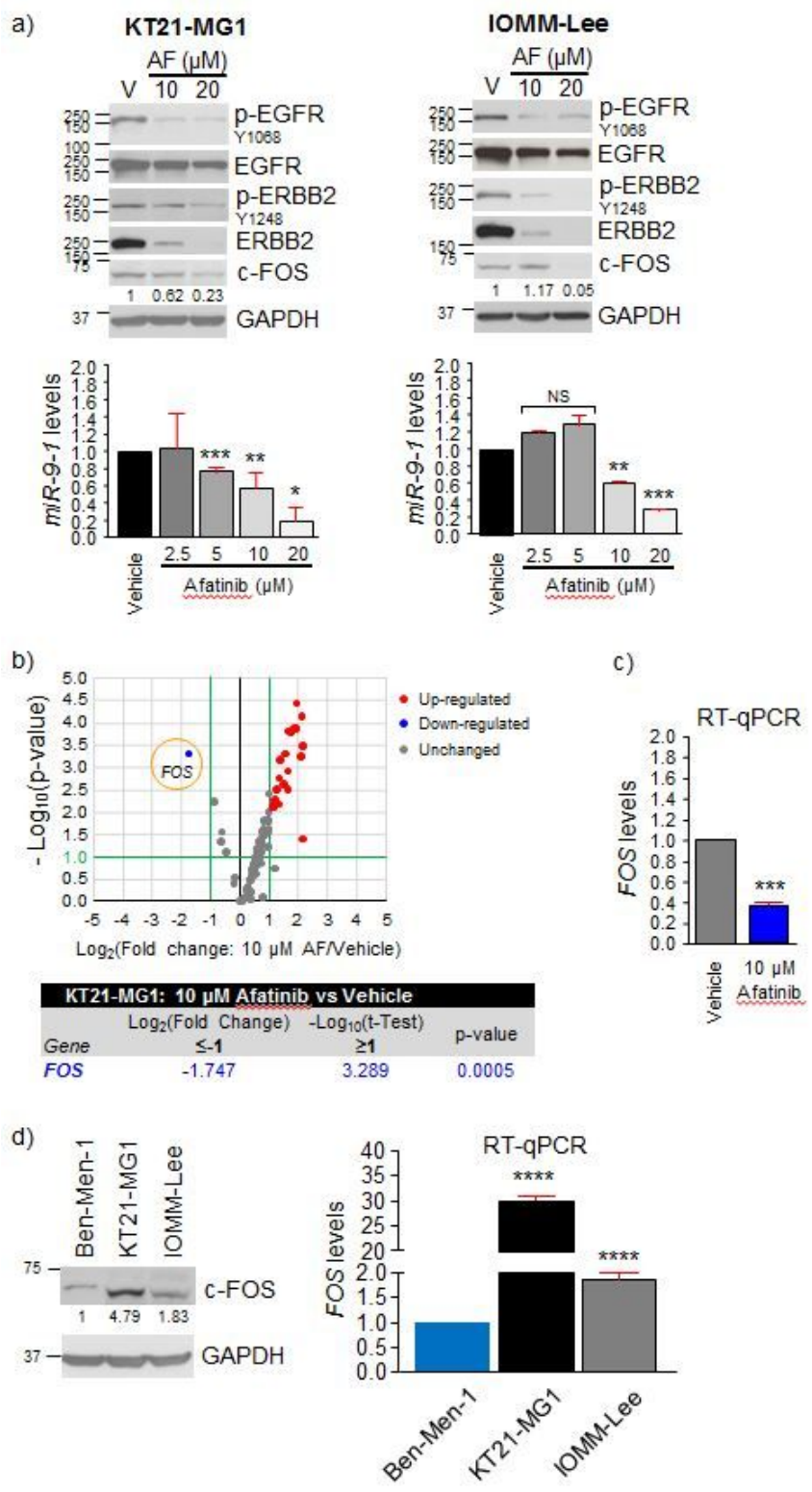

Figure 2

FOS is downregulated in malignant meningioma cells after Afatinib administration resulting in decreased miR-9-1 levels. a) KT21-MG1 and IOMM-Lee cells were treated with 10 and 20 μM of Afatinib, and EGF receptor inhibition was assayed within 24 hours (by following EGFR and ERBB2-Her2 receptors phosphorylation levels). Following Afatinib administration, FOS levels (representative Western blot and densitometry are reported) decreased in both KT21-MG1 and IOMM-Lee, followed by a significant

decrease of miR-9-1 in both malignant cell lines in a dose-response fashion, when compared to vehicle DMSO (at 20 μM Afatinib: 0.17 and 0.27 folds in KT21-MG1 and IOMM-Lee, respectively, see figures below Western blot panels). Data are expressed as mean ± SEM, ANOVA one-way (*p<0.05, **p<0.005, ***p<0.001), when compared to vehicle. b) Volcano plot reporting the RT2 profiler EGF-PDGFR RT-qPCR array performed by profiling the malignant KT21-MG1 (n=3) meningioma cells treated with 10 μM (from cell culture media) Afatinib versus vehicle (DMSO). Among all genes profiled, FOS was the only gene significantly downregulated in KT21-MG-1 cells treated with Afatinib at the indicated concentration (0.30 folds, p=0.00051, threshold p□0.01), when compared to vehicle DMSO. Green lines represent arbitrary threshold levels. c) RT-qPCR assay of FOS conducted in KT21-MG1 (n=3) meningioma cells after treatment with 10 μM Afatinib validated decreasing of FOS (0.36 folds, n=3) observed with the RT2 profiler EGF-PDGFR array, when compared to vehicle control. Data are expressed as mean ± SEM, ANOVA one-way (***p<0.001), when compared to vehicle. d) Representative analysis of FOS levels monitored by Western blot and RT-qPCR analysis in KT21-MG1 and IOMM-Lee cell lines, when compared to Ben-Men-1 cells. As reported, FOS is upregulated both at the protein and mRNA levels in the malignant meningioma cell lines (30.04 folds, KT21-MG1; 1.84 folds, IOMM-Lee). Data are expressed as mean ± SEM, ANOVA one-way (****p<0.001), when compared to Ben-Men-1 cells. All cell lines were profiled at three different passages, to ensure gene expression consistency.

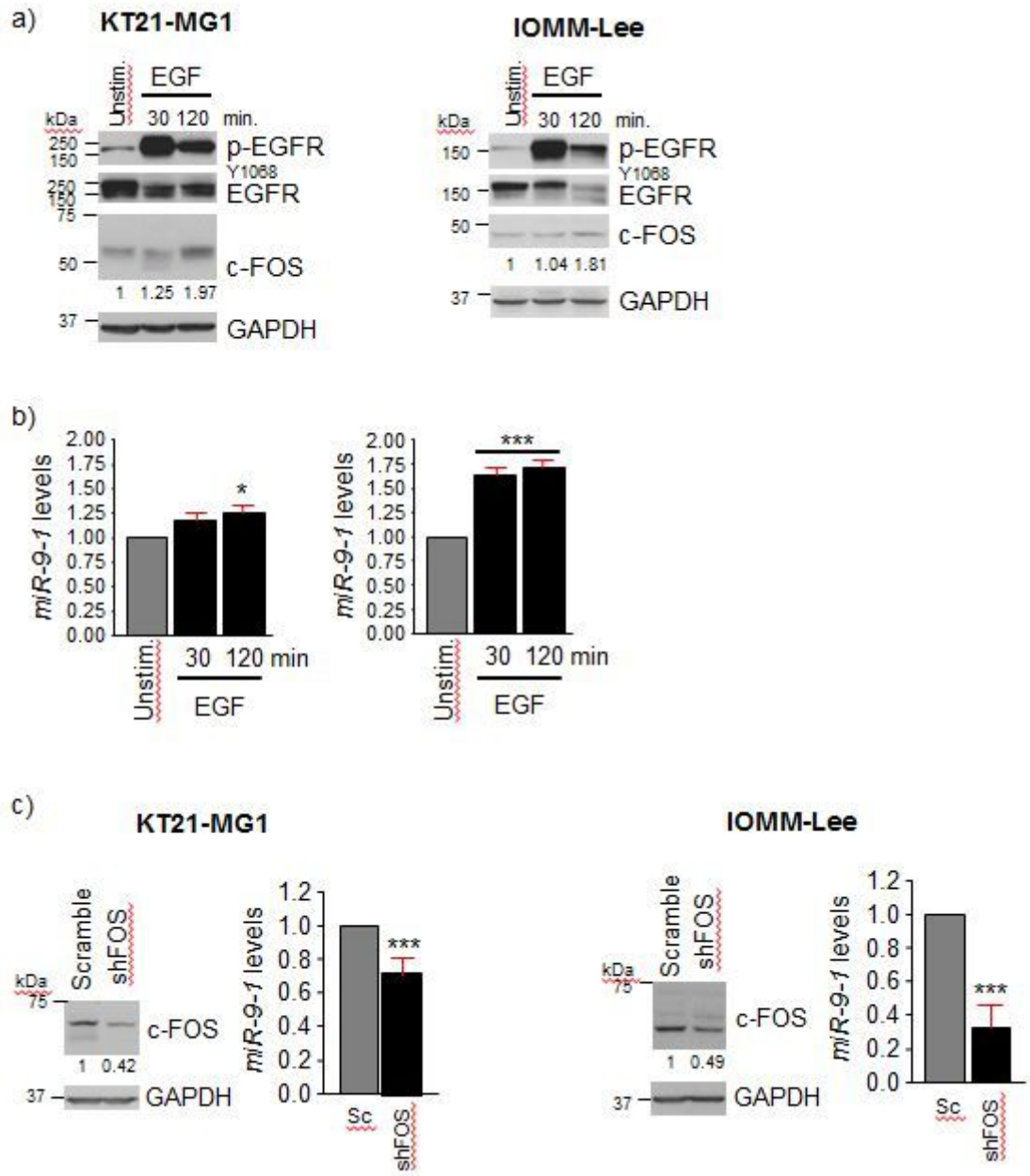

Figure 3

MiR-9-1 expression is controlled by FOS via stimulation of the EGFR pathway. a) KT21-MG1 and IOMM-Lee cells were treated with EGF, and receptor stimulation was assayed at the indicated time points. As reported by representative Western blots, EGF stimulation increased the protein levels of FOS both in KT21-MG1 and IOMM-Lee cells (when compared to unstimulated cells). b) Stimulation of the EGFR receptor was achieved using EGF in a time-course assay, and miR-9-1 was profiled by RT-qPCR. A significant increase of miR-9-1 levels was detected in both KT21-MG1 (1.18 and 1.26 folds) and IOMM-Lee (1.65 and 1.73 folds) by RT-qPCR analysis. Data are expressed as mean ± SEM, ANOVA one-way (*p<0.05, ***p<0.001), when compared to unstimulated cells. c) Achieved lentivirus-mediated RNA interference (n=2) of FOS in both KT21-MG1 and IOMM-Lee cells (assessed by following the FOS protein levels by Western blotting), was paralleled by a significant decrease of miR-9-1 levels in both malignant

cell lines (0.72 and 0.32 folds, respectively), when compared to scramble (assayed by RT-qPCR analysis). Data are expressed as mean ± SEM, ANOVA one-way (***p<0.005) when compared to scramble. The RNA interference was repeated twice, ensuring consistency.

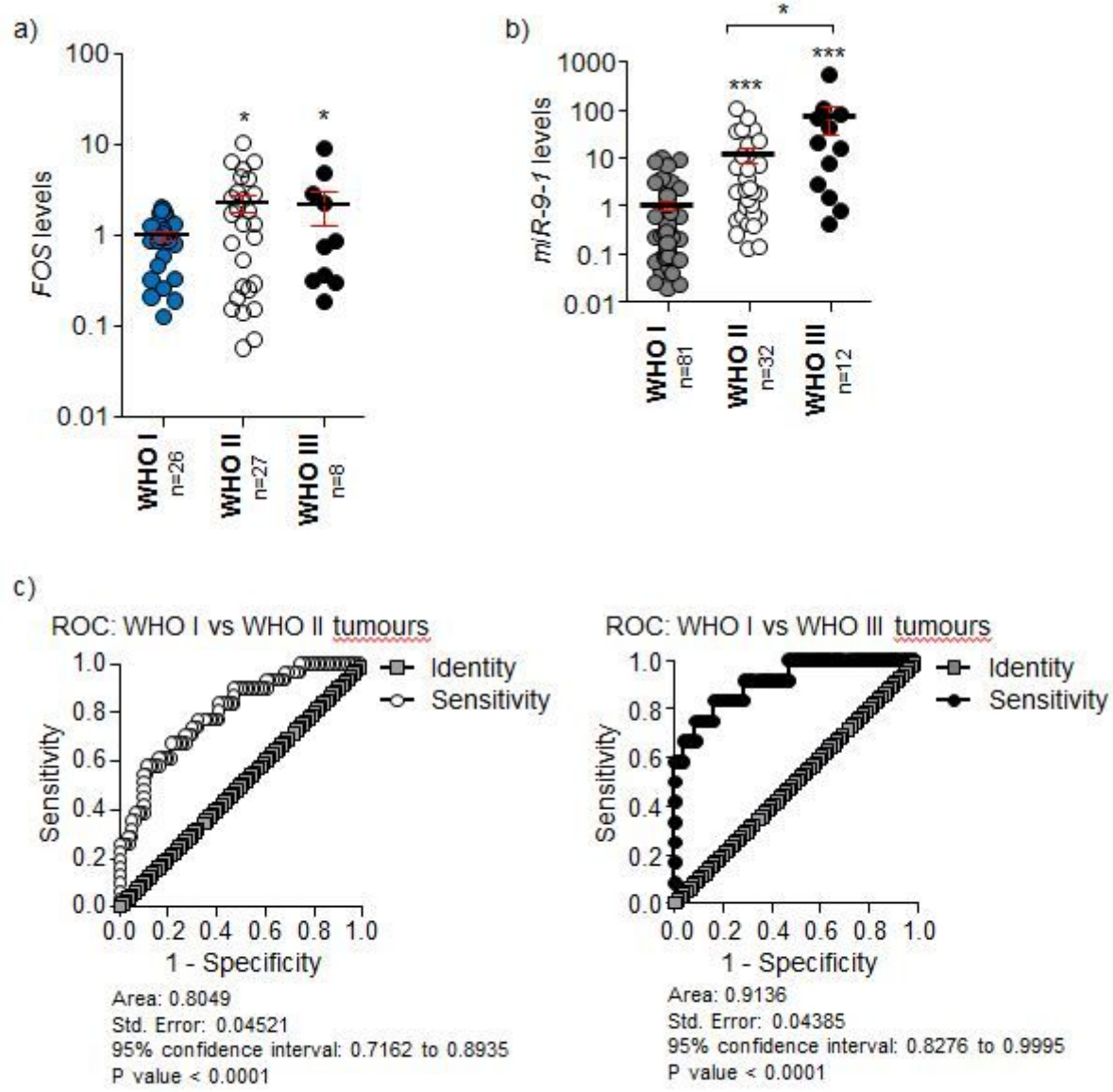

Figure 4

FOS and miR-9-1 are overexpressed in higher-grade meningioma. a) Gene expression analysis by RT-qPCR of FOS in meningioma tissues is reported. FOS showed a significant increase in WHO II (n=27, 2.26 Log10 folds) and III (n=8, 2.16 Log10 folds) tumors when compared to WHO I specimens (n=26). b) Gene expression analysis conducted by RT-qPCR of miR-9-1 in meningioma tissues showing its significant increase in WHO II (n=32, 11.56 Log10 folds) and III (n=12, 71.63 Log10 folds) tumors when compared to WHO I specimens (n = 81). c) Receiver operating characteristic (ROC) curve analysis of miR-9-1 in WHO II versus WHO I meningioma tumors (AUC=0.8049, p<0.0001, 95% confidence interval 0.7162 to 0.8935)

and WHO III versus WHO I (AUC=0.9136, p<0.0001, 95% confidence interval 0.8276 to 0.9995), is reported. Data are expressed as mean ± SEM, Student's t-Test (*p<0.05, ***p<0.001), when compared to WHO I tumors.

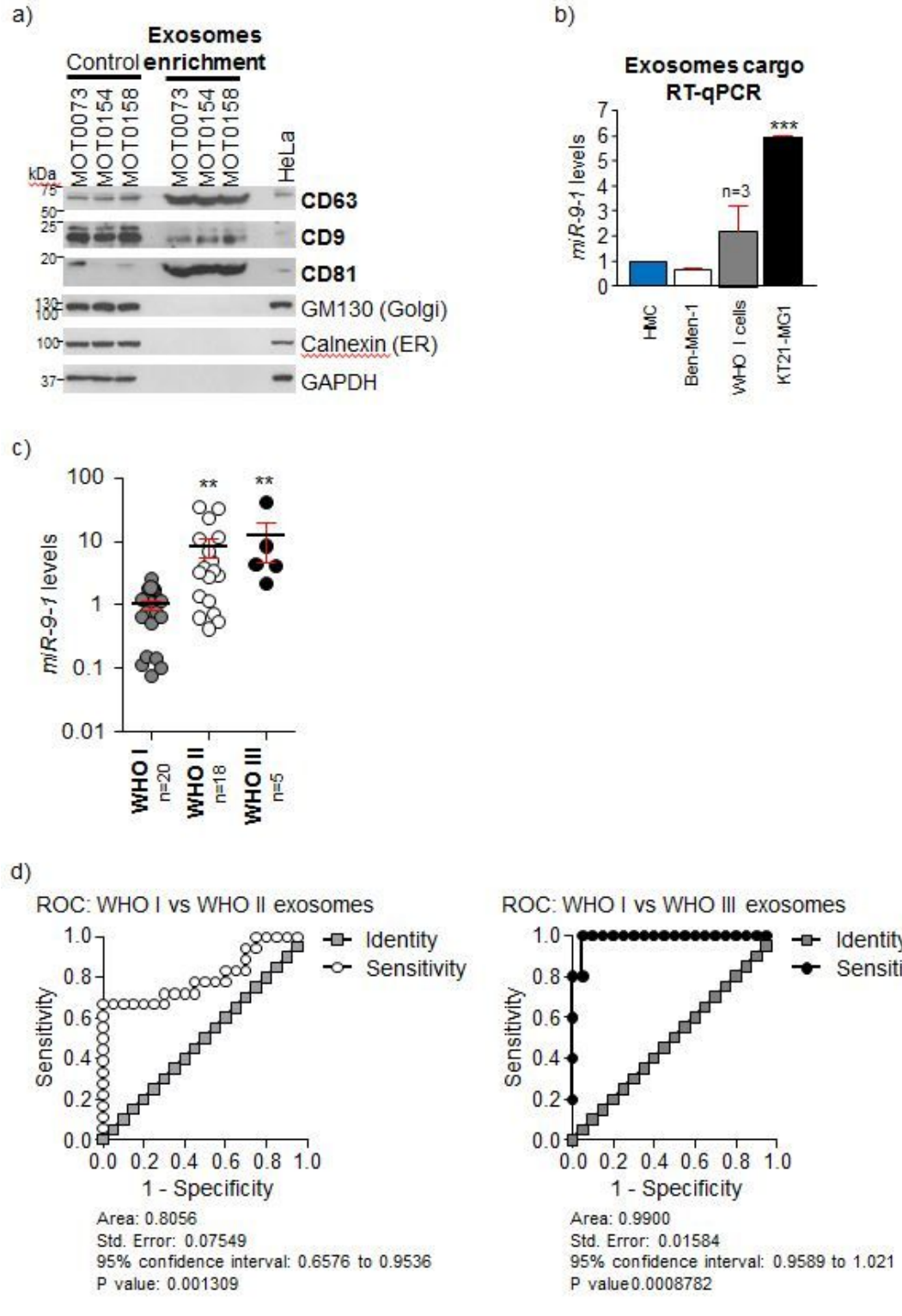

Figure 5

miR-9-1 is upregulated in higher-grade meningioma cargo in vitro, and in meningioma patient's serum exosomes. a) Exosome enrichment assay in vitro conducted by monitoring exosome biomarkers (CD63,

CD9 and CD81) by Western blotting demonstrates their enrichment in vitro, when compared to control (whole cell culture lysates). HeLa=positive control. b) RT-qPCR analysis of miR-9-1 shows its significant upregulation in exosomes released from KT21-MG1 (5.92 folds), when compared to Ben-Men-1 (0.66 folds) and tumor-derived WHO I cells (2.16 folds). Data are expressed as mean ± SEM, ANOVA one-way (***p<0.001), compared to HMC. The analysis was performed in biological triplicates to ensure data consistency. c) Analysis of miR-9-1 expression by RT-qPCR in circulating exosomes is reported. MiR-9-1 is significantly upregulated in WHO II (n=18, 8.10 Log10 folds) and WHO III (n=5, 11.99 Log10 folds) when compared to WHO I (n=20) meningioma patients. Data are expressed as mean ± SEM, Student's t-Test (**p<0.005), when compared to WHO I tumors. d) ROC curve analysis shows a high diagnostic value for miR-9-1 when comparing benign (WHO I) to atypical (WHO II) meningioma patients (AUC=0.8056, p<0.001309, 95% confidence interval 0.6576 to 0.9536) and a high diagnostic value when comparing benign (WHO I) to anaplastic (WHO III) meningioma patients (AUC=0.9900, p<0.0008782, 95% confidence interval 0.9589 to 1.021).

Supplementary Files

This is a list of supplementary files associated with this preprint. Click to download.

- BaizetalDatasetS3.xlsx
- BaizetalDatasetS2.xlsx
- BaizetalAdditionalfile3.xlsx
- BaizetalmiR91Additionalfile2.pptx
- BaizetalAdditionalfile1.xlsx